Variations in temperature and salinity of the surface water above the middle Okinawa Trough during the past 37 kyr

Hua Yu^{a, b, *}, Zhenxia Liu^b, Serge Berné^c, Guodong Jia^d, Yingqian Xiong^e, Gerald R. Dickens^a, Gangjian Wei^d, Xuefa Shi^b, J.Paul Liu^f and Fajin Chen^d

^a Department of Earth Sciences, Rice University, Houston, Texas, United States

^b First Institute of Oceanography, State Oceanic Administration, Qingdao, China

^c IFREMER, Geosciences Marines, Plouzane, France

^d Guangzhou Institute of Geochemistry, Chinese Academy of Sciences, Guangzhou, China

^e Department of Geosciences, University of Houston, Houston, Texas, United States

^f Department of Marine Earth and Atmospheric Sciences, North Carolina State University, Raleigh, North Carolina, United States

*: Corresponding author : Hua Yu, Tel.: +1 281 777 6780, email address : yuhua77@gmail.com

Abstract:

East China Sea (ECS) is an important climate modulator of East Asia. In the last glacial period, the global sea level, the path and strength of the Kuroshio Current experienced great changes; combined with the variable volume of fresh run-off input, they made the hydrographic situation in the ECS quite different from nowadays. Based on high-resolution alkenone-sea surface temperature (SST) and oxygen isotope composition of planktonic foraminifera Globigerinoides sacculifer we reconstructed paleo-sea surface salinity (SSS) of a long piston core DGKS9604 retrieved from the middle Okinawa Trough of the eastern ECS. The δ^{18} O and SST records display significant variations with global ice volume. Synchrony of the millennial-scale climate events like YD and Heinrich events of core DGKS9604 to the ice core from the northern high latitudes, and the synchroneity of deglacial warming with the Bølling-Allerød warming suggests a strong coupling of the SST variations in the marginal Pacific Ocean to the climate of the North Atlantic, most likely through the Asian monsoon atmospheric circulation. The ECS documents lowest SST (22 °C) at ~ 26 cal kyr BP and ~ 3 °C SST difference between the full glaciation (26 to 19 cal kyr BP) and mid-to-late Holocene (6 cal kyr BP-present). The overall long-term hydrographic variations in the middle Okinawa Trough are controlled by temporal and spatial variations in: (i) the intensity and position of the Kuroshio Current, (ii) intensity of the Asian summer monsoon and (iii) sea-level fluctuations coupled with ECS topography. Saline surface water dominated over the middle Okinawa Trough during early pre-glaciation (37 to 31 cal kyr BP), last deglaciation (19 to 11.6 cal kyr BP), and mid-to-late Holocene (6 cal kyr BP-present), whilst freshened surface water prevailed during the late pre-glaciation (31 to 26 cal kyr BP). full glaciation (26 to 19 cal kyr BP) and early Holocene (11.6 to 6 cal kyr BP).

Keywords: East China Sea; Okinawa Trough; Kuroshio Current; East Asian monsoon; Sea surface temperature; Sea surface salinity

38 **1. Introduction**

Okinawa Trough, a primary focus of this study, is a long (1200 km), crescent-shaped, 39 northeast trending back-arc basin located in the southeast portion of the East China Sea (ECS) 40 (Fig. 1). Connected with the open Pacific Ocean through seaways along the eastern margin, this 41 area is sensitive to the global climate, sea level variations as well as local environmental changes. 42 43 The current hydrographic situation of the Okinawa Trough are featured by the interaction 44 between warm, saline Western Boundary Current, Kuroshio Current, from the east side and cold, and fresh coastal water supplied by larges rivers, specially the Changjiang (Yangtze) river, from 45 the west side of China continents (Fig. 1) (e.g., Bryden et al., 1991; Hsueh, 2000; Tseng et al., 46 2000; Qiao et al., 2006; Itoh and Sugimoto, 2008; Andres et al., 2008; Nakano et al., 2008). 47 However, the local hydrographic situation during past climate regimes remains an outstanding 48 49 issue.

The present-day hydrography of the ECS must have been different during the last glacial 50 51 period. Because eustatic sea level was ~120 m lower in last glacial maximum (LGM) (e.g., 52 Hanebuth et al., 2000), and the ECS continental shelf has a low morphological gradient (about 58"), most of sea floor on the continental shelf was exposed. Major rivers (e.g. Changjiang, 53 Minjiang and Qiantangjiang) also advanced further seaward (Wellner and Bartek, 2003), likely 54 debouching large volumes of water and sediment onto the outer continental shelf and into the 55 Okinawa Trough. The magnitude and location of the Kuroshio Current also changed greatly 56 (Ujiié and Ujiié, 1999; Ujiié et al., 2003; Xu and Oda, 1999; Li et al., 2001; Ijiri et al., 2005). 57 Variations in the oceanography of the ECS should affect sea surface temperature (SST) and sea 58

59 surface salinity (SSS) of the Okinawa Trough.

Previous discussions of these two parameters in this region have relied primarily on the 60 assemblages of planktonic foraminifera, the δ^{18} O of planktonic foraminifera, or both (Ujiié and 61 Ujiié, 1999; Jian et al., 2000; Li et al., 2001; Ujiié et al., 2003). Because each proxy suffers from 62 certain kinds of biases, such as growth seasonality, preservation, diagenetic degradation, 63 64 calibrations, etc, a multiproxy reconstruction is justified (Mix et al., 2001; Bard, 2001). In this study, we generate high-resolution alkenone-sea surface temperature (SST) and $\delta^{18}O$ records of 65 Globigerinoides sacculifer for a long piston core from the western slope of the middle Okinawa 66 67 Trough to examine changes in annual mean SST and SSS for the past 37 kyrs, and discuss the mechanisms controlling the local hydrographic variations in the ECS. 68

69

70 2. Regional Setting

71 2.1 East China Sea

The ECS is a large $(7.7 \times 10^5 \text{ km}^2)$ marginal sea in the western Pacific Ocean bordered by mainland China, the Korean Peninsula, and the islands of Taiwan, Kyushu and Ryukyu (**Fig. 1**). It extends about 1300 km from northeast to southwest, and about 740 km from east to west. The seafloor of the ECS can be conveniently divided into three general bathymetric regions: the continental shelf (generally < 120 m water depth, mwd), the shelf break (120-170 mwd) and the slopes and basin of Okinawa Trough (> 170 mwd). The continental shelf stretches up to 600 km across, making it the widest such feature in eastern Asia.

79 The Okinawa Trough has resulted from the collision of the Philippine and Eurasian plates

(Sibuet et al., 1998). Although active today, rifting began from the middle to late Miocene (~ 6
Ma; Shinjo et al., 1991). Consequently, the geometry of the Okinawa Trough has been fairly
similar over the late Pleistocene. At present, the Okinawa Trough deepens from the northern
(~900 mwd) to southern region (~2700 mwd). Previous work indicates that a >1 km-thick
sedimentary sequence since late Miocene drapes the trough (Ishibashi et al., 1995).

85 Several prominent rivers contribute large amounts of water and sediment to this marginal sea (Fig. 1). Changjiang River, the fourth longest in the world, discharges ~920 km³/yr of water 86 and ~4.8 \times 10¹¹ kg/yr of sediment into the ECS (Milliman and Meade, 1983). Minjiang and 87 Qiantangjiang Rivers discharge additional ~ 94 km³/yr water and ~14 \times 10⁹ kg/yr sediment 88 (Zhang, 1995). The fresh water input lowers SSS and changes hydrographic characteristics of 89 water masses in the region, especially on the continental shelf (Beardsley et al., 1985). Given the 90 broad modern continental shelf, coastal processes distribute and deposit most of the fluvial 91 sediment around the river mouths and on the inner shelf; relatively small amounts of terrigenous 92 93 sediment reach the Okinawa Trough at present.

Fluvial discharge into the ECS varies greatly with seasons because of the East Asian monsoon variation and the shift of intertropical convergence zone (ITCZ). In winter, ITCZ shifts southward, cold and dry Siberian (continental) air masses flow with a direction to the southeast from inner Asia to the ocean. In summer, ITCZ shifts northward, warm and humid air masses flow in northwest direction from the Pacific and Indian Oceans. This leads to enhanced precipitation to the Chinese mainland in summer season. Consequently, approximately 70% of the annual discharge of the Changjiang River occurs between May and October (Chen et al., 101 2001).

102

103 2.2 Kuroshio Current

The Kuroshio Current is the major western boundary current in the North Pacific (Fig. 1). 104 The modern Kuroshio Current generally flows northeast above the Okinawa Trough (Fig. 1) as a 105 106 water mass up to 100 km wide and 800 to 1000 m deep. This current originates near the Equator and enters the ECS from the Philippine Sea through the Suao-Yonaguni Depression. It returns to 107 the North Pacific through Tokara Strait and merges with the North Pacific Current at roughly 37° 108 109 N off the Japan coast. The velocity of the current varies both regionally and seasonally, ranging from 45 to 150 cm/s (Qin et al., 1987). The flux of the Kuroshio Current also changes over time, 110 particularly with the El Niño Southern Oscillation. Strong transport occurs during La Niña years 111 112 when trade winds intensify, and weak transport occurs during El Niño years (Wyrtki, 1975; Qiu and Lukas, 1996). Typical water flux ranges from 21 to 33 Sv (Sverdrup, 1 Sv= 10^6 m³/s) 113 114 (Roemmich and McCallister, 1989; Johns et al., 2001).

The temperature and salinity on the ECS continental shelf and slope are controlled by the mixing of the continental run-off and the Kuroshio Current waters, resulting in a gradient that rises from the inner shelf to the shelf edge (Zhang et al., 1990).

118

119 **3. Materials and methods**

120 *3.1 Sediment core*

121 Piston core DGKS9604 was recovered by *R/V L'ATALANTE* from the middle Okinawa

122	Trough in 1996 during the joint Chinese-French DONGHAI cruise. The core site was chosen in
123	this study because seismic profiles showed thick packages of sediment with little evidence for
124	turbidites. Core DGKS9604 is 10.76 m long, and was recovered up the slope (28°16.64' N,
125	127°01.43' E) at 766 mwd (Fig. 1). It comprises homogeneous gray clayey silt, but has no ash
126	layers (Fig. 2). The core was cut into 1 m-long sections (excepting the short bottoms), then split,
127	described and sampled every 2 cm over the upper 100 cm, and every 4 cm below.

129 *3.2 Laboratory analyses*

Bulk sediment samples from core DGKS9604 were split into several aliquots for various analyses. Planktonic foraminifera shells were extracted from a set of sediment aliquots and analyzed for their isotopic compositions. Bulk sediment samples were washed through a 63 µm sieve and dried in an oven at 60 °C. Between 17 and 37 mg of planktonic foraminifera *Neogloboquadrina dutertrei* from 10 intervals and one planktonic foraminiferas mixture from the very bottom were picked for radiocarbon analyses at the National Ocean Sciences Accelerator Mass Spectrometry facility, Woods Hole Oceanographic Institution (**Table 1**).

Stable oxygen isotope was analyzed at a resolution of 2 cm through the upper portion of the core (0-100 cm), 4 cm through the middle interval of the core (100-600 cm), and 12 cm through the basal section (600- 1076 cm). Between 15 and 20 specimens of *G sacculifer* (without the sac-like final chamber) in the 300~350 μ m size fractions were collected under microscope. All tests were washed with ethanol in an ultrasonic bath, dried at 60°C, and measured at the Laboratory of Isotope Geochronology and Geochemistry, Guangzhou Institute of Geochemistry, Chinese Academy of Sciences using a GV IsoPrime stable isotope mass spectrometer. Results are
presented using standard delta notation (‰) relative to Vienna Pee Dee Belemnite (VPDB)
(Table 2). The analytical precision is better than ±0.08‰ for oxygen isotopes.

A third set of aliquots was stored in a cold room at -4 °C and subsequently processed for 146 alkenone measurements. Following procedures of Villanueva et al. (1997), freeze-dried samples 147 148 were homogenized with an agate mortar and pestle (~4 g), spiked with an internal standard of 149 *n*-hexatriacontane, and placed in an ultrasonic bath with dichloromethane. Extracts were then hydrolyzed with 6% potassium hydroxide in methanol to remove terrigenous wax esters. 150 151 Non-acidic compounds were recovered by extraction with *n*-hexane and elution by 8:2 dichloromethane-n-hexane in columns packed with 2 g silica. The collected solvents were 152 evaporated under a nitrogen stream and re-dissolved with 20 µl n-hexane. They were then 153 154 analyzed using an HP 6890 gas chromatograph equipped with a cold on-column injector system, a fused silica capillary column, and a flame ionization detector (FID). Helium, at a flow rate of 155 156 1.6 ml/min, was used as carrier gas. Oven temperature was programmed at 100 °C for 3 minutes (min), raised to 240 °C at a rate of 10 °C /min, raised to 295 °C at a rate of 2.5 °C /min and then 157 kept isothermal at 295 °C for 50 min. Alkenones were identified based on their retention times 158 and their concentrations were determined by comparing FID responses to known internal 159 160 standard concentrations (Fig. 3).

161

162 *3.3 Chronology*

163

For core DGKS9604, radiocarbon ages less than 20 kyr were converted to calendar ages

(cal kyr BP) using the CALIB 4.4 program (Stuiver et al., 1998). Radiocarbon ages older than 20 164 kyr were converted to calendar ages with the 'Fairbanks0805' calibration curve (Fairbanks et al., 165 2005) (**Table 1**). The age model for core DGKS9604 was initially derived by linear interpolation 166 between 10 of the 11 corrected radiocarbon ages (Table 1; Fig. 2). These datum occur in 167 reasonable stratigraphic order, and indicate deposition over the last 37 kyrs. The radiocarbon age 168 169 from 520-522 cm below the seafloor (cmbsf) is too young compared to surrounding intervals, suggesting sediment disturbance by bioturbation or mass wasting. Although turbidites were not 170 observed in this core, small turbidite layers have been found in other cores from the Okinawa 171 172 Trough (Li et al., 2003). In any case, this age has been ignored in the construction of the age model. 173

On the basis of this stratigraphy, apparent sedimentation rates generally decrease from late glaciation toward the present (**Fig. 2**). In core DGKS9604 the sediment accumulation rates vary from an average of ~40 cm/kyr during the late glaciation to an average of ~20 cm/kyr during the last deglaciation and the Holocene. The age resolution for successive samples in this core is about 100-300 yrs, significantly higher than those in cores from previous studies of the middle Okinawa Trough (Ujiié and Ujiié, 1999; Ujiié et al., 2003).

180

Two long-chain C_{37} methyl alkenones were found in core DGKS9604: $C_{37:2Me}$ (containing 2 double bonds) and $C_{37:3Me}$ (containing 3 double bonds). $C_{37:4Me}$ (methyl alkenones containing 4 double bonds) was not detected in any sample (**Fig. 3**).

¹⁸¹ *3.4 SST reconstruction*

The relative proportions of unsaturated C_{37} methyl alkenones are related to SST (e.g., Brassell et al., 1986; Prahl and Wakeham, 1987; Müller et al., 1998). A commonly used expression for the C_{37} alkenone abundance is the degree of ketone unsaturation (U_{37}^{k}), calculated as:

$$U_{37}^{k} = (C_{37:2Me} - C_{37:4Me}) / (C_{37:2Me} + C_{37:3Me} + C_{37:4Me}), \qquad (1)$$

Because $C_{37:4 \text{ Me}}$ is generally produced at low temperatures and accounts for only small part of the total ketone concentration, this index (**Eqn. 1**) is often simplified to (Prahl and Wakeham, 192 1987):

193
$$U_{37}^{k'} = C_{37:2Me} / (C_{37:2Me} + C_{37:3Me}).$$
(2)

A linear relationship between $U_{37}^{K'}$ and SST is apparent for most of the modern ocean between 60°N and 60°S where temperatures range from 0 °C to 29 °C (Prahl and Wakeham, 1987; Müller et al., 1998). A global core-top calibration for this relationship is (Müller et al., 1998):

197
$$SST = (U_{37}^{k'} - 0.044) / 0.033.$$
 (3)

We have applied equations (2) and (3) to alkenone determinations of samples from core DGKS9604 (**Table 2**). The core-top (0-1 cmbsf) for core DGKS9604 gives a SST of 26.2 °C, which compares favorably to the present-day annual mean SST at this location of 25.7 °C within the error estimate (**Table 3**). The replicate measurements of alkenone show that uncertainties (\pm 1 σ) for $U_{37}^{K'}$ are \pm 0.006, thus, \pm 0.2 °C for SST.

203

204 3.5 SSS reconstruction

205 Planktonic foraminiferal oxygen isotope records can be used to reconstruct past SSS if (1)

206 the SST component of the signal can be "removed", (2) global salinity variations resulted from 207 changes in ice volume can be "subtracted", and (3) the oxygen isotope composition of ambient 208 water co-varied with salinity predictably (Schmidt et al., 2006; Weldeab et al., 2006; Toledo et al., 209 2007). For *G Sacculifer*, water temperature (*T* in °C) relates to δ^{18} O as follows (Erez and Luz, 209 1983):

211
$$T = 17.0 - 4.52(\delta^{18}O_c - \delta^{18}O_w) + 0.03(\delta^{18}O_c - \delta^{18}O_w)^2, \qquad (4)$$

212 where the subscripts c and w refer to test calcite and seawater, respectively.

Waelbroeck et al. (2002) presented a detailed global mean ocean $\delta^{18}O_w$ record that spans the last four glacial-interglacial cycles. This record suggests a 1.05‰ decrease in mean $\delta^{18}O_w$ from the LGM to the Holocene. Oba (1990) has shown a linear relationship between SSS and $\delta^{18}O_w$ for the region of the ECS influenced by the Kuroshio Current (Eqn. 5, **Fig. 4**):

217
$$\delta^{18}O_w = 0.203 \text{ SSS} - 6.76$$
. (5)

Assuming the relationship between SSS and $\delta^{18}O_w$ has been constant through the last glacial-interglacial cycle, Equations 4 and 5 enable fairly precise SSS records to be calculated from alkenone SST and foraminiferal $\delta^{18}O_c$ records by subtracting the global salinity signal.

221

222 **4. Results**

223 4.1 Sea surface temperature trends

The *G.sacculifer* δ^{18} O and alkenone SST records from core DGKS9604 display significant variations with global ice volume and strong coherency with each other (**Fig. 5**). This suggests that water chemistry and SST have changed in phase with global ice volume during the last 227 glacial-interglacial cycle, an observation made at many locations.

The basal part of core DGKS9604 shows small fluctuations in the SSTs that seem to 228 229 stabilize around 23.5°C from 37 to 31 cal kyr BP (calibrated thousands of years before present, i.e., 1950 AD), which we refer as the "early pre-glaciation" (Fig. 5E). A large cooling peaked 230 around 30.5 cal kyr BP appears contemporaneous with the North Atlantic Heinrich event 3 (H3); 231 the δ^{18} O shifted 1‰ heavier and the SSTs dropped 1-2 °C (Fig. 5B, D, E). Then the SST 232 reversed gradually, culminating in peak warmth to ~24°C at 27 cal kyr BP. SSTs subsequently 233 dropped, reaching minimum temperature over our study interval at ~26 cal kyr BP about 22°C. 234 235 Following the minimum SSTs, the surface water above the middle Okinawa Trough sustained cold through the full glacial time interval (26-19 cal kyr BP). Comparing with the late Holocene 236 the SSTs over study site dropped ~3°C in the LGM (Fig. 5E). This long-term glacial duration 237 possibly suggest the lowest glacial sea level has reached at ca.26 cal kyr BP in the ECS, which is 238 consisted with records from Barbados Island (Peltier and Fairbanks, 2006). Whilst this long-term 239 240 cold interval was culminated by a large cooling event near 21.5 cal kyr BP, coeval with H2 in North Atlantic (Fig. 5E). The surface water started to warm slowly during the first deglacial 241 phase and was terminated by a cooling event happened at ca. 17-15.4 cal kyr BP, which 242 documented ~1°C SST drop and corresponded to H1 event recorded in Greenland ice cores (Fig. 243 244 **5E**). Contemporaneous with the Bølling/Allerød warming recorded in high latitudes of the northern hemisphere the SSTs over our study site, in phase with the *G.sacculifer* δ^{18} O records, 245 began to increase rapidly at ca.14.7 cal kyr BP, synchronous with the melt water pulse - 1A 246 (MWP-1A) (Fig. 5A, E), marking the second half of the last deglaciation. It was terminated by a 247

major cooling event, peaked around ~11.6 cal kyr BP, synchronous with the North Atlantic YD cold event (**Fig. 5**). In the early Holocene, from 11.6 to 8.5 cal kyr BP the SSTs over site DGKS9604 increased abruptly, accomplishing the ultimate recovery from the YD cold reversion. A cooling event around 8.2 cal kyr BP was documented both in SSTs and *G.sacculifer* δ^{18} O records, which has been discussed in detail by Yu et al. (2007). In mid and late Holocene since 6 cal kyr BP, the SSTs stabilized at 26°C.

254

255 *4.2 Sea surface salinity trends*

The accuracy of the SSS records warrants commentary because, unlike other studies using 256 Mg/Ca (e.g., Schmidt et al., 2006; Weldeab et al., 2006), the SST and $\delta^{18}O_c$ records have been 257 determined on different phases made by different organisms. In particular, coccolithophorids and 258 G. sacculifer have different growing seasons in ECS. Sediment trap studies in the eastern ECS 259 demonstrate that the flux of coccoliths to the sea floor is high throughout the year with the 260 exception of summer months (Tanaka, 2003), whereas the flux of G. sacculifer shells is high 261 throughout the year with the exception of winter months (Yamasaki and Oda, 2003; Xu et al., 262 2005). However, both organisms grow prosperously in spring and fall, when most surface water 263 properties, including SST and SSS, approach annual averages (**Table 3**). Therefore, $U_{37}^{K'}$ -derived 264 SSTs could be a good candidate to be used to obtain accurate average SSSs in the region. 265 What's more, reconstructed SSS for core DGKS9604 averaging at 34.4‰ during the Late 266 Holocene (0-6 cal kyr BP) matches very well with instrument measured present-day annual 267 average SSS of 34.51±0.23‰ at the core site (Table 3). 268

SSS records over site DGKS9604 generally fluctuate with high amplitude (Fig. 5F), which 269 is partially caused by the point-to-point calculation of individual δ^{18} O and alkenone SST values. 270 271 However this does not preclude making general comments about the trend of these oscillations by soothing the record (Fig. 5F). During the early pre-glacial period, from 37 to 31 cal kyr BP 272 the SSSs stabilized at ca. 34‰ in core DGKS9604. Following the high early pre-glacial SSS, a 273 274 long-term low SSS excursion peaked around 28 cal kyr BP with SSS dropping up to 5%. This seems synchronous with the Dansgaard-Oeschger (D-O) cycle 3 and/or 4 (Dansgaard et al., 1993) 275 (Fig. 5B, F). A decreasing SSS trend persisted from 26 to 19 cal kyr BP throughout the full 276 277 glaciation (Fig. 5F). Over the early last deglaciation, from 19 to 14.7 cal kyr BP, an obvious increasing trend was observed in the core, comparing with a clear decreasing trend between 14.7 278 and 11.6 cal kyr BP. In early Holocene, from 11.6 to 6 cal kyr BP, a prominent decrease trend in 279 salinity was documented. SSSs dropped up to 3-4‰ during this time interval. In Mid-to-late 280 Holocene (6 cal kyr BP to present) the SSSs increased to stabilize at 34.4‰ over site core 281 282 DGKS9604.

283

284 **5. Discussion**

The accuracy of the reconstructed paleo-SSS records in this study suffered from 1) assumption of constant SSS - $\delta^{18}O_w$ relationship in the last glacial period, 2) low temporal resolution of the global sea water $\delta^{18}O_w$, and 3) slight different habitats for planctonic foraminifera and phytoplankton. Bearing this in mind, we will not go too far to discuss every single blip in detail in SSS curves associated with short-term climate events like Heinrich, YD and 8200 cooling event here. We pay more attention on long-term hydrographic evolution in thispaper.

292

293 5.1 Pre-glaciation

During early pre-glaciation, from 37 to 31 cal kyr BP, the average SSS for core DGKS964 294 295 was almost as the same as the modern situation (Fig. 5F). As to temperature the SSTs in the middle Okinawa Trough at that time were about 23 to 24 °C (Fig. 5E), just a little colder than 296 present-day. Local paleoclimate studies based on different archives indicated a very humid 297 climate in early pre-glaciation (Shi and Yu, 2003); the precipitation brought by the Asian summer 298 monsoon in southeast China was as high as that of late Holocene as suggested by the 299 speleotheme δ^{18} O record (Yuan et al., 2004, **Fig. 5C**). Large transgressions occurred in the ECS, 300 301 where the sea level was only 2.5-12.25 m lower than the present-day sea level, much lower than the global estimation of 20-40 m (Chappell et al., 1996) due to local tectonic subsidence (Yang et 302 303 al., 2004; Zhao et al., 2008). In our study site a tremendous high sedimentation rate, ~70 cm/kyr occurred during 33 to 31 cal kyr BP in core DGKS9604 (Fig. 2), which could correspond to 304 maximum transgression in the ECS. This high stand could partially facilitate large volume of 305 warm and saline Kuroshio Current penetrated through Suao-Yonaguni Depression in our study 306 area and kept this slight saline surface water high persisting over the middle Okinawa Trough for 307 about 7 kyrs. Additionally high Asian summer monsoon would make the North Equatorial 308 Current (NEC) bifurcation position shift southward (Qiu and Lukas, 1996), and the Kuroshio 309 Current extended deeper (Qu and Lukas, 2003), both resulting in a significant amount of warm 310

311 and salty equatorial water transported toward the pole.

However during the late pre-glaciation the timing of SST, $\delta^{18}O$ and SSS between core 312 313 DGKS9604 and north Greenland ice core was quite complicated. Most notably, at the termination of H3 SST oscillated with high frequencies, but a consistent and obvious decreasing 314 salinity trend was documented in our records, which centered around 28-29 cal kyr BP (Fig. 5E, 315 316 F). This possibly indicated the influence of strong Asian summer monsoon in response to the warm stadial period D-O 3 and/or 4 in North Atlantic (Fig. 5B, C). Large precipitation brought 317 by the Asian summer monsoon could lead this low SSS anomaly. However more high-resolution 318 319 paleoclimate records of this time interval are needed to reveal the mechanism of this SSS excursion. 320

321

322 5.2 Full glacial period

During the full glacial interval (26-19 cal kyr BP) the SSTs over study site were as low as 323 22°C, dropped ~3°C comparing with the late Holocene (Fig. 5E). This is consistent with records 324 from other cores in this area (Xiong and Liu, 2004; Ijiri et al., 2005; Sun et al., 2005; Zhou et al., 325 2007). Although there are some high SSS bumps, a decreasing trend in SSS curve was observed 326 during this period (Fig. 5F). This could be explained by the more easterly position of the river 327 drainage systems on the exposed shelf and/or reduced Kuroshio Current intensity. A significant 328 sea-level fall of ~120 m during the LGM (Chappell et al., 1996; Hanebuth et al., 2008) have 329 exerted great influences on the paleoceanographic environment variation in the middle Okinawa 330 Trough. Due to the low morphological gradient of the ECS continental shelf the coastline 331

advanced seaward hundreds of kilometers during the low stand. Thus the position of the river 332 plume was more proximal to the core site (Wellner and Bartek, 2003). Therefore a larger volume 333 of fresh water would have entered our study sites although less precipitation and less absolute 334 discharge of the Yangtze River into the ECS was probably deduced by decreased Asian summer 335 monsoon as implied by the Chinese speleotheme records (An et al., 1991; Wang and Sun, 1994; 336 337 Yuan et al., 2004). The enhanced fresh run-off at this time has been reported in the northern Okinawa Trough (Xu et al., 1999; Ijiri et al., 2005) as well as in the nearby core site DGKS9603 338 from geochemical evidences (Xiong and Liu, 2004). Additionally the path and strength of the 339 340 Kuroshio Current experienced great changes during this period (Ujiié and Ujiié, 1999; Ujiié et al., 2003; Xu and Oda, 1999; Li et al., 2001; Ijiri et al., 2005). This Current may have been reduced 341 greatly in intensity ((Xu and Oda, 1999; Ijiri et al., 2005) or completely prevented from entering 342 343 the ECS by a land bridge connecting the central and southern Ryukyu Arc with Taiwan. It could turned eastward south of the Ryukyu Arc, but not flowing above the Okinawa Trough during the 344 LGM (Ujiié and Ujiié, 1999, Ujiié 2003; Jian et al., 2000; Li et al., 2001). Reduced Kuroshio 345 Current intensity or complete shift-out of such current would be another important factor 346 resulting in this low salinity during full glaciation. 347

348

Synchronously with the LGM termination (19, 000 \pm 250 years, Yokoyama et al., 2000) the SSS over site DGK9604 reveals a clear increasing trend, especially between 19 and 14.7 cal kyr BP (**Fig. 5F**). The association of cold and extreme salty sea surface water in the early last

^{349 5.3} Last deglaciation

deglaciation could be explained by the coupling variations in the Kuroshio Current and the Asian 353 summer monsoon intensity. At the termination of LGM, continental ice volume decreased rapidly 354 by about 10%, which resulted in a rapid sea level rise of 10-15 m, namely 19-kyr MWP (Fig. 5A) 355 (Yokoyama et al., 2000; Clark et al., 2004; Hanebuth et al., 2008). This could enhance the 356 throughflow of salty Kuroshio Current in the middle Okinawa Trough due to the disappearance 357 358 of the topographic high blocks at LGM low stand. Whilst at this time interval the winter monsoon was still in very strong intensity and summer monsoon was weakened further (Fig. 5C), 359 this more arid climate could boost the remarkably saline hydrographic condition at the first phase 360 of last deglaciation over study area. 361

Synchronous with Bølling-Allerød warming in the North Atlantic at 14.7 cal kyr BP both 362 $U_{37}^{K'}$ -SST and δ^{18} O show abrupt warming of surface water in the trough area, corresponding to a 363 quick reversal of strong Asian summer monsoon (Fig. 5B, C, D, E). This agrees with many 364 observations in the East Asian marginal seas like the South China Sea (Review see Kiefer and 365 Kienast, 2005). It suggests a close coupling of the SST variations to the climate of the North 366 Atlantic through the atmospheric circulation. Although the absolute SSS values were still high, 367 there is a clear trend toward lower salinity over the late last deglaciation, between 14.7 to 11.6 368 cal kyr BP (Fig. 5F). By comparing with the Asian summer monsoon records (Fig. 5C) this 369 decreasing salinity could be caused by the gradually increased precipitation brought by the 370 enhanced summer monsoon. 371

It might be tempting to think that the excessively high absolute SSS value during the whole last deglaciation, especially from 16 to 11.6 cal kyr BP, is an artifact of outstandingly warm 374 alkenone SST estimates (Fig. 6A). However other temperature proxies revealed similar warm situation in the Okinawa Trough in the second half of last deglaciation (Fig. 6B, C). A nearby 375 core A7 (126°58.7' E, 27°49.2' N) show high SSTs around 25°C based on Mg/Ca ratios of 376 for a for a minifera G ruber (Fig. 6B) (Sun et al., 2005). Although not as well resolved as $U_{37}^{K'}$ and 377 Mg/Ca - SST records, SST reconstructions based on planktonic foraminiferal assemblage from 378 379 core DGKS9603 also show high temperature around 26°C in cold season and 28°C in warm season during the late last deglaciation (Fig. 6C) (Li et al., 2001). Those multiple proxies 380 corroborate the outstanding high sea surface temperature, therefore, high surface salinity during 381 382 the last deglaciation, indicating profound changes in oceanic conditions. We argue that the warming in the northern high latitudes, northward displacement of the ITCZ and strengthening of 383 northeast trade winds during more La Niña-like last deglacial conditions induced an 384 intensification of heat and salinity transport associated with the Kuroshio Current (Koutavas et 385 al., 2002). Both high SST and SSS values occurred at 16 cal kyr BP, possibly suggesting the 386 387 restoration of high intensity Kuroshio Current in the middle Okinawa Trough could achieve fulfillment at 16 cal kyr BP after LGM. Since then warm and saline surface water dominated 388 over the trough area (Fig. 5E,F). This point is also supported by paleoceanographic evidences 389 from core DGKS9603 (Li et al., 2001). Heat and salt release from the Kuroshio Current may 390 have accelerated and amplified warming around the East Asia continent, especially the Japanese 391 Archipelago. 392

393

394 5.4 Low sea surface salinity in early Holocene

395	Since early Holocene, from 11.6 to 6 cal kyr BP, a long-lived salinity decreasing was
396	observed over the middle Okinawa Trough (Fig. 5F). One plausible explanation for this
397	long-term decrease in SSS by 3-4‰ is supreme precipitation associated with high intensity in
398	Asian summer monsoon at this interval, which is clearly evidenced by oxygen isotope of
399	stalagmite formations in caves from southeast China (Fig. 5C) (Wang et al., 2001; Yuan et al.,
400	2004; Dykoski et al., 2005). This low SSS may also suggest weakened Kuroshio Current
401	associated with strong El Niño activities in early Holocene, as documented in Peruvian sea
402	(Carré et al., 2005; Wang and Hu, 2006).
403	Followed this long-term salinity low, the SSS increased gradually from 6 cal kyr BP. It is
404	well corresponding to the colder and dryer climate in the mid-to-late Holocene. Southward shift
405	of ITCZ and weakened Asian summer monsoon could be the major factors inducing such climate,
406	therefore surface oceanography in our study area (Wanner et al., 2008).
407	
408	6 Conclusion
408 409	6 Conclusion Although there are some uncertainties inherent with the reconstructed paleo-SSS records in
409	Although there are some uncertainties inherent with the reconstructed paleo-SSS records in
409 410	Although there are some uncertainties inherent with the reconstructed paleo-SSS records in this study, combination of SST, SSS and other evidences allow some key conclusions to be
409 410 411	Although there are some uncertainties inherent with the reconstructed paleo-SSS records in this study, combination of SST, SSS and other evidences allow some key conclusions to be drawn about the long-term hydrographic variations in the middle Okinawa Trough.
409 410 411 412	Although there are some uncertainties inherent with the reconstructed paleo-SSS records in this study, combination of SST, SSS and other evidences allow some key conclusions to be drawn about the long-term hydrographic variations in the middle Okinawa Trough. (1) The SST variation pattern over long sedimentation sequence in the middle Okinawa

416 monsoon system.

(2) Persistent and pronounced cooling prevailed in the middle Okinawa Trough for the time
interval from ~26 to 19 cal kyr BP. It possibly indicated the lowest sea level have already taken
placed at 26 cal kyr BP in the ECS, which is suggested by Peltier and Fairbanks (2006) at the
island of Barbados.

421 (3) The SST difference between the full glaciation and late Holocene is $\sim 3^{\circ}$ C in the ECS.

422 (4) The SSS was low at the full glaciation, which could be contributed to the proximal
423 position of the continental river plume and reduced Kuroshio Current intensity.

(5) The SSS started to increase at 19 cal kyr BP, synchronous with the 19-kyr sea level rise.
The pulse-like sea level rise might have played a crucial role in the restoration of high intensity
Kuroshio Current in the middle Okinawa Trough. The fulfillment of the restoration of this
current could achieve on 16 cal kyr BP, when warm and saline surface water dominated the
middle Okinawa Trough.

(6) The outstanding decreasing salinity trend since the late deglaciation (~14.7 cal kyr BP),
especially persisted and eminent low SSS in the early Holocene, from 11.6 to 6 cal kyr BP,
indicated strong controlling of the Asian summer monsoon on the hydrographic situation over
area circum-continental slope. This observation is first reported in the middle Okinawa Trough
so far.

434 (7) Overall the long-term hydrographic variations in the middle Okinawa Trough are
435 mainly driven by an interaction of the intensity and position of the Kuroshio Current, intensity of
436 the Asian summer monsoon and sea level fluctuations coupled with topography.

438 Acknowledgements

We are grateful to the crew of DONGHAI cruise of R/V L'Atalante in the ECS in 1996 for their support in sampling core DGKS9604. We thank Glen Snyder and Micah Nicolo for helpful remarks and language corrections. We also are indebted to two anonymous reviewers for their constructive comments on this paper. This work was funded by joint Chinese-French project supported by the NSFC (Grant No. 40421150011), MOST (Grant No. 2003cb716706) and NSF, China (Grant No. 40431002). The DONGHAI cruise was funded by IFREMER.

445

446 **References**

- 447 An, Z., Kukla, G.J., Porter, S.C., Xiao, J., 1991. Magnetic susceptibility evidence of monsoon
- variation of the Loess Plateau of Central China during the last 130,000 years. Quaternary
 Research 36, 29-36.
- 450 Andres, M., Park, J.H., Winibush, M., Zhu, X., Chang, K., Ichikawa, H., 2008. Study of the
- 451 Kuroshio/Ryukyu Current System Based on Satellite-Altimeter and in situ measurements.

452 Journal of Oceanography 64 (6), 937-950.

- 453 Bard, E., 2001. Comparison of alkenone estimates with other paleotemperature proxies.
- 454 Geochemistry, Geophysics, Geosystems, doi: 2000GC000050.
- 455 Beardsley, R.C., Limeburner, R., Yu, H., Cannon, G.A., 1985. Discharge of the Changjiang
- 456 (Yangtze River) into the East China Sea. Continental Shelf Research 4, 57-76.
- 457 Brassell, S.C., Brereton, R.G., Eglinton, G., Grimalt, J., Liebezeit, G., Marlowe, I.T., Pflaumann,

458	U., Broecker, W.S, 1986. Oxygen isotope constraints on surface ocean temperatures.
459	Quaternary Research 26, 121-134.
460	Bryden, H.L., Roemmich, D.R., Church, J.A., 1991. Ocean heat transport across 24°N in the
461	Pacific. Deep-Sea Research 38, 297-324.
462	Carré, M., Bentaleb, I., Fontugne, M., Lavallée, D., 2005. Strong El Niño events during the early
463	Holocene: stable isotope evidence from Peruvian sea shells. The Holocene 15, 42-47.
464	Chappell, J., Omura, A., Esat, T., McCulloch, M., Pandolfi, J., Ota, Y., Pillans, B., 1996.
465	Reconciliation of late Quaternary sea levels derived from coral terraces at Huon Peninsula
466	with deep sea oxygen isotope records. Earth Planet Science Letter 141, 227-236.
467	Chen, X., Zong, Y., Zhang, E., Xu, J., Li, S., 2001. Human impacts on the Changjiang (Yangtze)
468	River basin, China, with special reference to the impacts on the dry season water discharges
469	into the sea. Geomorphology 41, 111-123.
470	Clark, P.U., McCabe, A.M., Mix, A.C., Weaver, A.J., 2004. Rapid rise of sea level 19,000 years
471	ago and its global implications. Science 304, 1141-1144.
472	Dansgaard, W., Johnson, S.J., Clausen, H.B., Dahl-Jensen, D., Gundestrup, N.S., Hammer, C.U.,
473	Hvidberg, C.S., Steffensen, J.P., Sveinbjörnsdottir, A.E., Jouzel, J., Bond, G., 1993.
474	Evidence for general instability of past climate from a 250 kyr ice-core record. Nature 364,
475	218-220.
476	Dykoski, C.A., Edwards, R.L. Cheng, H., Yuan, D., Cai, Y., Zhang, M., Lin, Y., Qing, J., An, Z.,
477	Revenaugh, J., 2005. A high-resolution, absolute-dated Holocene and deglacial Asian
478	monsoon record from Dongge Cave, China. Earth and planetary science letter 233, 71-86.

- 479 Erez, J., Luz, B., 1983. Experimental paleotemperature equation for planktonic foraminifera.
 480 Geochimica et Cosmochimica Acta 47, 1025-1031.
- 481 Fairbanks R.G., Mortlock R.A., Chiu T.C., Cao L., Kaplan A., Guilderson T.P., Fairbanks T.W.,
- 482 Bloom A.L., Grootes P.M., Nadeau M.J., 2005. Radiocarbon calibration curve spanning 0 to
- 483 50,000 years BP based on paired 230 Th/ 234 U/ 238 U and 14 C dates on pristine corals.
- 484 Quaternary Science Reviews 24, 1781-1796.
- 485 Grootes, P. M., Stuiver, M., White, J. W. C., Johnsen, S. J., Jouzel, J., 1993. Comparison of
- 486 oxygen isotope records from the GISP2 and GRIP Greenland ice cores. Nature 366,
- 487 552-554.
- Hanebuth T., Stattegger K., Grootes P.M., 2000. Rapid flooding of the Sunda Shelf: a late-glacial
 sea-level record. Science 288, 1033-1035.
- 490 Hanebuth, T.J.J., Stattegger, K., Bojanowski, A., 2008. Termination of the Last Glacial
- 491 Maximum sea-level lowstand: The Sunda-Shelf data revisited. Global and Planetary Change
- 492 doi: 10.1016/j.gloplacha.2008.03.011.
- 493 Hsueh Y., 2000. The Kuroshio in the East China Sea. Journal of Marine Systems 24, 131-139.
- 494 Ijiri, A., Wang, L., Oba, T., Kawahata, H., Huang C.Y., Huang C.Y., 2005. Paleoenvironmental
- 495 changes in the northern area of the East China Sea during the past 42,000 years.
- 496 Palaeoceanography, Palaeoclimatology, Palaeoecology 219, 239-261.
- 497 Ishibashi J., Sano Y., Wakita H., Gamo T., Tsutsumi M., Sakai H., 1995. Helium and carbon
- 498 geochemistry of hydrothermal fluids from the Mid-Okinawa Trough back arc basin,
- 499 southwest of Japan. Chemical Geology 123, 1-15.

500	Itoh, S., Sugimoto, T., 2008. Current variability of the Kuroshio near the separation point from
501	the western boundary. Journal of Geophysics Research 113, C11020, doi:
502	10.1029/2007JC004682.
503	Jian, Z., Wang, P., Saito, Y., Wang, L., Pflaumann, U., Oba, T., Cheng, X., 2000. Holocene
504	variability of the Kuroshio Current in the Okinawa Trough, northwestern Pacific Ocean.
505	Earth and Planetary Science Letters 184, 305-319.
506	Johns, W.E., Lee, T.N., Zhang, D., Zantopp, R., 2001. The Kuroshio east of Taiwan: moored
507	transport observations from the WOCE PCM-1 array. Journal of Physical Oceanography 31,
508	1031-1053.
509	Kiefer, T., Kienast, M., 2005. Patterns of deglacial warming in the Pacific Ocean: a review with
510	emphasis on the time interval of Heinrich event 1. Quaternary Science Reviews 24,
511	1063-1081.
512	Koutavas, A., Lynch-Stieglitz, J., Marchitto, T.M., Sachs, J.P., 2002. El Niño-like pattern in Ice
513	Age tropical Pacific sea surface temperature. Science 297, 226-230.
514	Li, J., Gao, S., Sun, Y., Zeng, Z., 2003. Grain-size variation of terrigenous sediment sequences in
515	the South Okinawa Trough (in Chinese with English abstract). Acta Sedimentologica Sinica
516	21, 461-466.
517	Li, T., Liu, Z., Hall, M., Berne, S., Saito, Y., Cang, S., Cheng, Z., 2001. Heinrich event imprints
518	in the Okinawa Trough: evidence from oxygen isotope and planktonic foraminifera.
519	Paleogeography Paleoclimatology Paleoecology 176, 133-146.
520	Liu, Z., Li T., Li P., Huang, Q., Cheng, Z., Wei, G., Liu L., Li, Z., Berne, S., Saito, Y., 2001. The

- paleoclimatic events and cause in the Okinawa Trough during 50 ka BP. Chinese Science
 Bulletin 46, 153-157.
- Milliman, J. D., Meade, R.C., 1983. World-wide delivery of river sediment to oceans. Journal of
 Geology 91, 1-21.
- Mix, A.C., Bard, E., Schneider, R., 2001. Environmental processes of the ice age: land, ocean,
 glaciers (EPILOG). Quaternary Science Reviews 20, 627-657.
- 527 Müller P.J., Kirst G., Ruhland G., Storch, I.V., Melé, A.R., 1998. Calibration of the alkenone
- 528 paleotemperature index U_{37}^{k} based on core-top from the eastern South Atlantic and the

529 global ocean (60°N~60°S). Geochimica et Cosmochimica Acta 62, 1757-1772.

- 530 Nakano, H., Tsujino, H., Furue, R., 2008. The Kuroshio Current system as a jet and twin
- ⁵³¹ "relative" recirculation gyres embedded in the Sverdrup circulation. Dynamics of
- 532 Atmospheres and Oceans, 45, 135-164.
- 533 Oba, T., 1990. Paleoceanographic information obtained by the isotopic measurement of
- individual foraminiferal specimens. Proc. First China Int. Conf. Oceanic Asian Mar. Geol.,169-180.
- 536 Peltier, W.R., Fairbanks, R.G., 2006. Global glacial ice volume and Last Glacial Maximum
- duration from an extended Barbados sea level record. Quaternary Science Reviews 25,
 3322-3337.
- 539 Prahl, F.G., Wakeham, S.G, 1987. Calibration of unsaturation patterns in long-chain ketone
 540 compositions for paleotemperature assessment. Nature 330, 367-369.
- 541 Qiao, F., Yang, Y., Lv, X., Xia, C., Chen, X., Wang, B., Yuan, Y., 2006. Coastal upwelling in the

- 542 East China Sea in winter. Journal of Geophysical Research 111,
- 543 doi:10.1029/2005JC003264.
- ⁵⁴⁴ Qin, Y., Zhao, Y., Chen, L., Zhao, S., (ed) 1987. Geology of the East China Sea (in Chinese).
- 545 Beijing, Science Press, P6.
- 546 Qiu, B., Lukas, R., 1996. Seasonal and interannual variability of the North Equatorial Current,
- 547 the Mindanao Current, and the Kuroshio along the Pacific western boundary. Journal of
- 548 Geophysical Research 101, 12315-12330.
- 549 Qu, T., Lukas, R., 2003. The bifurcation of the North Equatorial Current in the Pacific. Journal of
- 550 Physical Oceanography 33, 5-18.
- ⁵⁵¹ Roemmich, D., McCallister, T., 1989. Large scale circulation of the North Pacific Ocean.
- 552 Progress in Oceanography 22, 171-204.
- 553 Schmidt, M.W., Vautravers, M.J., Spero, H.J., 2006. Rapid subtropical North Atlantic salinity
- oscillations across Dansgaard-Oeschger cycle. Nature 443, 561-564.
- 555 Shi, Y., Yu, G., 2003. Warm-humid climate and transgressions during 40~30 ka B.P. and their
- 556 potential mechanisms (in Chinese with English abstract). Quaternary Sciences 23, 1-11.
- 557 Shinjo, R., Ban, M., Saito, K., Kato, Y., 1991. K-Ar dating of the volcanic rocks in the Ryukyu
- arc (in Japanese, with English abstract). J. Jpn. Assoc. Miner. Petrol. Econ. Geol. 86,
- *323-328.*
- 560 Sibuet, J. C., Deffontaines, B., Hsu, S. K., Thareau, N., Formal J. P. L., Liu, C. S., ACT party,
- 561 1998. Okinawa trough backarc basin: Early tectonic and magmatic evolution. Journal of
- 562 Geophysical Research 103, B12, 30,245- 30,267.

563	Stuiver, M., Reimer, P.J., Braziunas, T.F., 1998. High-precision radiocarbon age calibration for
564	terrestrial and marine samples. Radiocarbon 40, 1127-1151.
565	Sun, Y.B., Oppo, D.W., Xiang, R., Liu, W., Gao, S., 2005. Last deglaciation in the Okinawa
566	Trough: Subtropical northwest Pacific link to Northern Hemisphere and tropical climate.
567	Paleoceanography 20, A4005. doi:10.1029/2004PA001061.
568	Tanaka, Y., 2003. Coccolith flux and species assemblages at the shelf edge and in the Okinawa
569	Trough of the East China Sea. Deep-Sea Research II: Topical Studies in Oceanography 50,
570	503-511.
571	Toledo, F.A.L., Costa, K.B., Pivel, M.A.G., 2007. Salinity changes in the western tropical South
572	Atlantic during the last 30 kyr. Global and Planetary Changes 57, 383-395.
573	Tseng C., Lin C., Chen S., Shyu C., 2000. Temporal and spatial variations of sea surface
574	temperature in the East China Sea. Continental Shelf Research 20. 373-387.
575	Ujiié, H., Ujiié, Y., 1999. Late Quaternary course changes of the kuroshio Current in the Ryukyu
576	Arc region, northwestern Pacific Ocean. Marine Micropaleontoloty 37, 23-40.
577	Ujiié, Y., Ujiié, H., Taira, A., Nakamura, T., Oguri, K., 2003. Spatial and temporal variability of
578	surface water in the Kuroshio source region, Pacific Ocean, over the past 21, 000 years:
579	evidence from planktonic foraminifera. Marine Micropaleontoloty 49, 335-364.
580	Villanueva, J., Pelejero, C., Grimalt, J. O., 1997. Clean up procedures for the unbiased estimation
581	of C_{37} alkenone sea surface temperatures and terregenous n-alkane inputs in
582	paleoceanography. Journal of Chromatography 757, 145-151.
583	Waelbroeck, C., Labeyrie, L., Michel, E., Duplessy, J.C., McManus, J.F., Lambeck, K., Balbon,

584	E., Labracherie, M., 2002. Sea-level and deep water temperature changes derived from
585	benthic foraminifera isotopic records. Quaternary Science Reviews 21, 295-305.
586	Wang Y.J., Cheng H., Edwards, R.L., An Z.S. Wu J.Y., Shen, C.C., Dorale, J.A., 2001. A
587	high-resolution absolute-dated late Pleistocene monsoon record from Hulu Cave, China.
588	Science 294, 2345-2348.
589	Wang, P., Sun, X., 1994. Last glacial maximum in China: comparison between land and sea.
590	Catena, 23, 341-353.
591	Wang, Q., Hu, D., 2006. Bifurcation of the North Equatorial Current derived from altimetry in
592	the Pacific Ocean. Journal of Hydrodynamics 18, 620-626.
593	Wanner, H., Beer, J., Bütikofer, J., Crowley, T.J., Cubasch, U., Flückiger, J., Goosse, H.,
594	Grosjean, M., Joos, F., Kaplan, J.O., Küttel, M., Müller, S.A., Prentice, I.C., Solomina, O.,
595	Stocker, T.F., Tarasov, P., Wagner, M., Widmann, M., 2008. Mid- to Late Holocene climate
596	change: an overview. Quaternary Science Reviews 27, 1791-1828.
597	Weldeab, S., Schneider, R.R., Kölling, M., 2006. Deglacial sea surface temperature and salinity
598	increase in the western tropical Atlantic in synchrony with high latitude climate instabilities.
599	Earth and Planetary Science Letters 241, 699-706.
600	Wellner, R.W., Bartek, L.R., 2003. The effect of sea level, climate, and shelf physiography on the
601	development of incised-valley complexes: a modern example from the East China Sea.
602	Journal of sedimentary research 73, 926-940.
603	Wyrtki, K., 1975. El Niño- the dynamic response of the Pacific Ocean to atmospheric forcing.
604	Journal of Physical Oceanography 5, 572-584.
	30

605	Xiong, Y., Liu, Z., 2004. The late Quaternary resource variation and its cause of the middle
606	Okinawa trough (in Chinese with English abstract). Acta Oceanologica Sinica 26, 61-71.
607	Xu, X., Yamasaki, M., Oda, M., Honda, M.C., 2005. Comparison of seasonal flux variations of
608	planktonic foraminifera in sediment traps on both sides of the Ryukyu Islands, Japan.
609	Marine Micropaleontology 58, 45-55.
610	Xu, X., Oda, M., 1999. Surface-water evolution of the eastern East China Sea during the last 36,
611	000 years. Marine Geology 156, 285-304.
612	Yamasaki M., Oda M., 2003. Sedimentation of planktonic foraminifera in the East China Sea:
613	evidence from a sediment trap experiment. Marine Micropaleontology 49, 3-20.
614	Yang, D., Chen, K., Shu, X., 2004. A preliminary study on the paleoenvironment during MIS 3 in
615	the Changjiang delta region (in Chinese with English abstract). Quaternary Sciences 24,
616	525-530.
617	Yokoyama Y., Lambeck K., Deckker P.D., Johnston P., Fifield L.K., 2000. Timing of the Last
618	Glacial Maximum from observed sea-level minima. Nature 406, 713-716.
619	Yu, H., Xiong, Y., Liu, Z., Berné, S., Huang, C., Jia, G., 2007. Evidence for the 8,200 a B.P.
620	cooling event in the middle Okinawa Trough. Geo-marine Letters 28(3), 131-136.
621	Yuan, D., Cheng, H., Edwards, R.L., Dykoski, C.A., Kelly, M.J., Zhang, M., Qing, J., Lin, Y.,
622	Wang, Y., Wu, J., Dorale, J.A., An, Z., Cai, Y., 2004. Timing, duration, and transitions of
623	the last interglacial Asian Monsoon. Science 304, 575-578.
624	Zhang, J., 1995. Geochemistry of trace metals from Chinese river/estuary systems: an overview.
625	Estuarine, Coastal and Shelf Science 41, 631-658.

626	Zhang, J., Letolle, R., Martin, J.M., Jusserand, C., Mouchel, J.M., 1990. Stable oxygen isotope
627	distribution in the Huanghe (Yellow River) and the Changjiang (Yangtze River) estuarine
628	systems. Continental Shelf Research 10, 369-384.
629	Zhao, B., Wang, Z., Chen, J., Chen, Z., 2008. Marine sediment records and relative sea level
630	change during late Pleistocene in the Changjiang delta area and adjacent continental shelf.
631	Quaternary International 186, 164-172.
632	Zhou, H., Li, T., Jia, G., Zhu, Z., Chi, B., Cao, Q., Sun, R., Peng, P., 2007. Sea surface
633	temperature reconstruction for the middle Okinawa Trough during the last
634	glacial-interglacial cycle using C_{37} unsaturated alkenones. Palaeogeography,
635	Palaeoclimatology, Palaeoecology 246, 440-453.
636	

636	Section 2: table caption
637	Table 1 AMS ¹⁴ C ages measured in core DGKS9604
638	
639	Table 2 δ^{18} O and SST records of core DGKS9604
640	
641	Table 3 Measured temperature and salinity of different seasons and annual average in study
642	area around 28°N, 127°E (data obtained from Japan Oceanographic Data Center database,
643	http://www.jodc.go.jp)
644	

644 Section 3: figure caption

Fig. 1 Regional map of the East China Sea and the Okinawa Trough. Location of core
DGKS9604 is represented by black bold circle. Reference cores, DGKS9603 (Liu et al., 2001),
Z₁₄₋₆ (Zhou et al., 2007), MD982195 (Ijiri et al., 2005), A7 (Sun et al., 2005) are represented by
gray bold circles. Shaded arrows represent the Kuroshio Current and its branches, small and
white arrows show fresh water discharge from the Chinese continent (after Xu et al., 2005).
SYD- Suao-Yonaguni Depression, TS - Tokara Strait.

651

Fig. 2 Lithology and chronology of core DGKS9604. Number beside hollow triangle
 represents calibrated AMS ¹⁴C ages with one-sigma range in parentheses. Sedimentation rates are
 also shown.

655

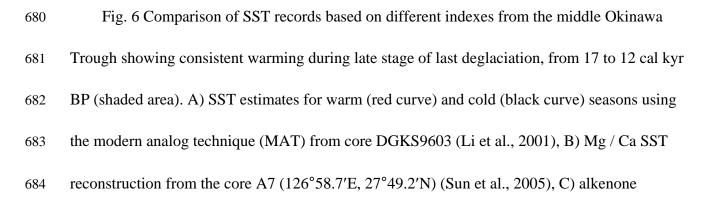
Fig. 3 A typical gas chromatogram showing the separation and retention times of alkanes and alkenones for a sample from the Holocene of core DGKS9604. C_{25} - C_{33} represent long-chain alkane peaks, $C_{37:2Me}$ and $C_{37:3Me}$ present the peaks for $C_{37:2}$ and $C_{37:3}$ alkenones. The C_{38} alkenone peaks are also shown here.

660

Fig. 4 Linear relationship between SSS and $\delta^{18}O_w$ in the region from ECS to the coast off the southern Japan influenced by the Kuroshio Current. This plot is drawn based on high accuracy measurements of SSS and $\delta^{18}O_w$ of seawater from 10 stations (modified after Oba, 1990).

Fig. 5 Comparison of the climate evolution in the middle Okinawa Trough with temperature 666 records from Greenland, Asian summer monsoon intensity and sea level. (A) Sea level rise at the 667 Sunder Shelf, Southeast Asia, in the last deglaciation (Hanebuth et al., 2000; Hanebuth et al., 668 2008); the blue bar depicts MWP-19kyr and MWP-1A. (B) $\delta^{18}O_{ice}$ of the GISP2 Greenland ice 669 core (Grootes et al., 1993). (C) Stacked stalagmite δ^{18} O from Hulu cave (Wang et al., 2001) and 670 Dongge Cave (Yuan et al., 2004) in which lighter peaks indicating high precipitation. (D) δ^{18} O 671 record of G sacculifer from core DGKS9604. (E) Alkenone-SST record of core DGKS9604. (F) 672 673 Reconstructed SSS of core DGKS9604. The red line is five-point average and the blue line represents the average SSS value of modern situation around 34.4‰. Climatic intervals are 674 abbreviated as follows: M-LH, Mid-to-late Holocene; EH, early Holocene; LLD, late last 675 deglaciation; ELD, early last deglaciation; FG, full deglaciation; LPG, late pre-glaciation; EPG, 676 early pre-glaciation; YD, Younger Dryas; BA, Bølling-Allerød; H1, Heinrich 1; H2, Heinrich 2; 677 H3, Heinrich3. Numbers depict Dansgaard-Oeschger cycles. 678

679



unsaturation index based SST reconstruction from the core DGKS9604 (green curve) of this

686 study.